

# Immobilization of carbon nanotubes on functionalized graphene film grown by chemical vapor deposition and characterization of the hybrid material

Prashanta Dhoj Adhikari<sup>1</sup>, Seunghan Jeon<sup>1</sup>, Myoung-Jun Cha<sup>1</sup>,  
Dae Sung Jung<sup>2</sup>, Yooseok Kim<sup>1</sup> and Chong-Yun Park<sup>1,2</sup>

<sup>1</sup> Center for Nanotubes and Nanostructured Composites, BK 21 plus Physics Research Division, Sungkyunkwan University, Suwon 440-746, Republic of Korea

<sup>2</sup> Department of Energy Science, Sungkyunkwan University, Suwon 440-746, Republic of Korea

E-mail: [cypark@skku.edu](mailto:cypark@skku.edu)

Received 21 May 2013

Accepted for publication 6 January 2014

Published 30 January 2014

## Abstract

We report the surface functionalization of graphene films grown by chemical vapor deposition and fabrication of a hybrid material combining multi-walled carbon nanotubes and graphene (CNT-G). Amine-terminated self-assembled monolayers were prepared on graphene by the UV-modification of oxidized groups introduced onto the film surface. Amine-termination led to effective interaction with functionalized CNTs to assemble a CNT-G hybrid through covalent bonding. Characterization clearly showed no defects of the graphene film after the immobilization reaction with CNT. In addition, the hybrid graphene material revealed a distinctive CNT-G structure and p-n type electrical properties. The introduction of functional groups on the graphene film surface and fabrication of CNT-G hybrids with the present technique could provide an efficient, novel route to device fabrication.

Keywords: chemical vapor deposition-grown graphene film, self-assembled monolayer, multi-walled carbon nanotubes, hybrid characterization


 Online supplementary data available from [stacks.iop.org/STAM/15/015007/mmedia](http://stacks.iop.org/STAM/15/015007/mmedia)

## 1. Introduction

Graphene has emerged as a new class of materials [1] that has attracted tremendous attention because of its remarkable physical, electrical and optical properties [2–6]. Such properties have encouraged studies of graphene for potential applications in solar cells, field-emission devices, field-effect transistors, supercapacitors and batteries [7–9]. Unfortunately, the configuration and manipulation of graphene is difficult owing to its hydrophobic nature [10], which remains a significant challenge for its utilization at the macroscopic

level [11]. In this context, functionalization of graphene film is important for controllable processing. As yet, most methods for ascribing molecules onto graphene have concentrated on non-covalent  $\pi$ -bond stacking [12] or have utilized graphene oxide (graphene sheets) [13–15].

In recent times, considerable effort has focused on the self-assembly and chemical modification of graphene films, in which most covalent functionalization experiments have typically relied on reactive diazonium salts [16], azides [17] or halogenation reactions [18, 19]. However, most of the above techniques suffer from a lack of active terminal group/property control, leading to inadequate handles for further chemical bonding to other materials (likewise; CNT). Moreover, graphene hybrid materials with interconnected networks may have superior durability/applicability features

 Content from this work may be used under the terms of the [Creative Commons Attribution-NonCommercial-ShareAlike 3.0 licence](http://creativecommons.org/licenses/by-nc-sa/3.0/). Any further distribution of this work must maintain attribution to the author(s) and the title of the work, journal citation and DOI.

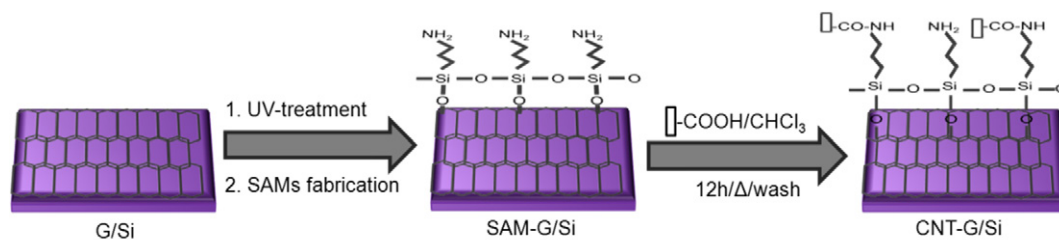


**Figure 1.** Schematic of the preparation process of surface-functionalized graphene film and fabrication of CNT-G hybrid material.

for use in flexible devices. Therefore, CNT immobilization onto functionalized CVD graphene film would be highly desirable for the establishment of uninterrupted CNT-graphene networks. To realize the merits of combined two-dimensional (2D) graphene and one-dimensional CNT nanocarbon materials, there have been many recent attempts to obtain graphene sheet-CNT hybrid materials or composites. For this instance, Yu and Dai [20] prepared a graphene sheet/CNT hybrid film with interconnected networks, for use in supercapacitors. In addition, attempts have been made to fabricate graphene sheet/CNT hybrid film by spin-coating homogeneously mixed solutions of the two carbon-based nanomaterials [21], as well as using a solid-phase layer stacking approach with ethanol wetting [22].

Here, we report a simple approach to activate CVD-grown graphene film through self-assembled monolayer (SAM) fabrication followed by UV treatment, which creates an efficiently oxidized film surface. To the best of our knowledge, the utility of UV-treatment for fabrication of SAM on CVD-grown graphene film and the preparation of CNT-G hybrid material through chemical bonding have not yet been reported. This method could be useful as a new route to the fabrication of graphene hybrid materials for a variety of potential applications.

## 2. Experimental details

### 2.1. Materials

HNO<sub>3</sub>, CHCl<sub>3</sub>, UV-lamp (Viber Lourmat, UV System, France), 3-aminopropyltriethoxysilane (APTES), 0.5 M FeCl<sub>3</sub> solution, toluene, ethanol, CNTs (ILJIN, Nanotech), cellulose membrane filter paper (1 μm pore size) and ultrasonicator (100 W, 60 Hz), were commercial products that were used as received. Deionized water was used in all experiments.

### 2.2. Preparation of CVD graphene film

Graphene was grown on copper (Cu) by atmospheric pressure CVD using methane as a carbon source. The reaction was carried out at 1050 °C for 20 min with a mixture flow of H<sub>2</sub>/methane of 100/10 sccm. After the reaction, the Cu foil was cooled to room temperature under an H<sub>2</sub> environment. To obtain free-standing graphene film, the Cu foil was etched with 0.5 M FeCl<sub>3</sub> solution. The detached graphene film was rinsed with deionized water and freely floating film on the water surface was transferred onto a SiO<sub>2</sub>/Si substrate (G/Si) [23].

### 2.3. Surface functionalization of graphene film

APTES solution was deposited onto G/Si in the vapor phase. Before the actual fabrication process, a pretreatment step was used to terminate the G/Si surface with OH groups. The pretreatment step involved UV-irradiation for 30 min (UV-G/Si). Then, a glass beaker containing the UV-treated G/Si and 1% APTES/toluene solution was placed in an air-tight steel box. The box was loaded into the processing chamber. Upon heating at 115 °C for 2 h, the silane precursor evaporated into the inner processing chamber space to create a saturated atmosphere consisting of coating molecules that reacted with the UV-G/Si to form SAM deposition. Next, the functionalized graphene was thoroughly sonicated for 10 s, rinsed with toluene and ethanol, and then dried under a stream of N<sub>2</sub> gas (SAM-G/Si).

### 2.4. Surface functionalization of carbon nanotubes

Acid functionalization of multi-walled carbon nanotubes (CNTs) was carried out by oxidation of CNTs with 60% HNO<sub>3</sub>. CNTs (30 mg) and HNO<sub>3</sub> (60 ml) were mixed in a flask equipped with a condenser. The mixture was heated to 80 °C overnight. The resulting CNTs were vacuum filtered, and rinsed with deionized water until the pH was neutral. This material was heated to 60 °C in a vacuum oven for 1 h.

### 2.5. Preparation of CNT-G hybrid material

The acid-treated CNTs were ultrasonically dispersed in chloroform solution. The SAM-G/Si substrate was immersed in the solution, and the reaction mixture was kept overnight at 45 °C. The substrate was then removed from the mixture, sonicated for 10 s and rinsed with ethanol to remove unabsorbed CNTs. The immobilized CNT on SAM-G/Si is referred to as CNT-G/Si (graphene hybrid material) and is shown in figure 1.

### 2.6. Characterization

Surface modified G/Si substrates were characterized by x-ray photoelectron spectroscopy (XPS). XPS spectra were obtained using a theta probe (VGMICROTEC, ESCA 2000) with a monochromatic AlKα source at a pressure of  $2 \times 10^{-9}$  mbar. Raman spectra were obtained using a Renishaw 1000 micro-Raman spectrometer at an excitation wavelength of 514 nm where at least three different sites on each sample were evaluated. Graphene topography before and after SAM fabrication was evaluated by an atomic force

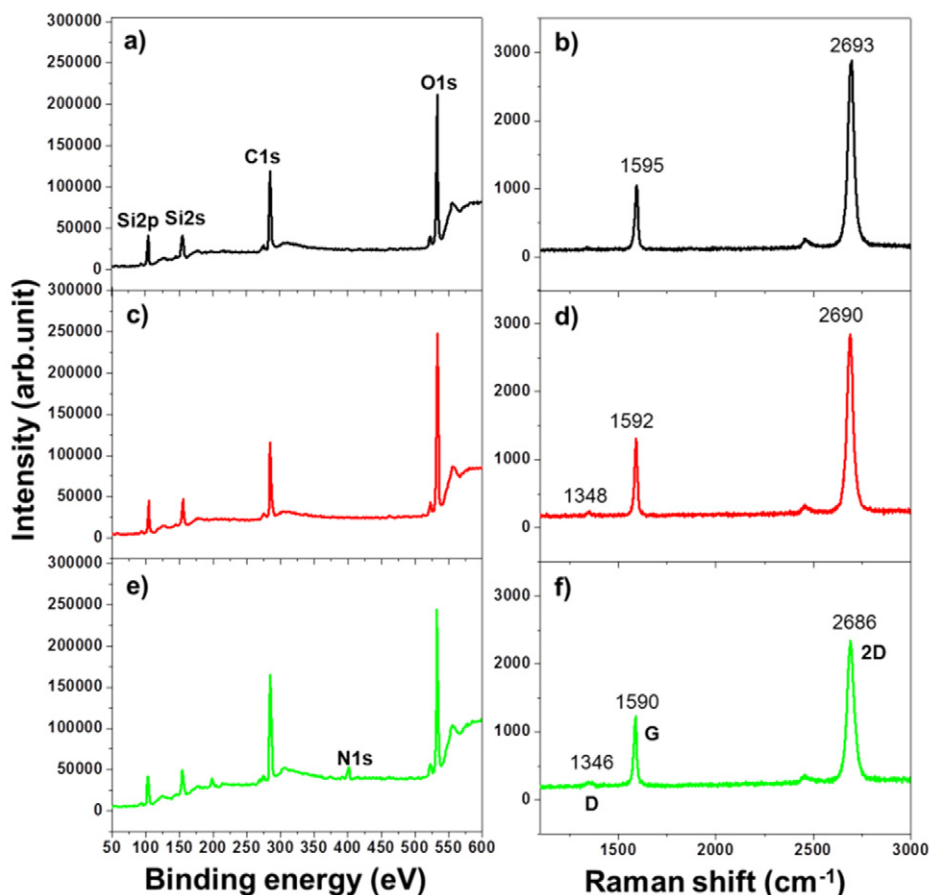


**Figure 2.** XPS survey spectra profile and Raman spectra for G/Si (a) and (b), UV-G/Si (c) and (d) and SAM-G/Si (e) and (f).

microscope (AFM, SPA 400). Fourier-transform infrared spectroscopy (FTIR, Bruker, IFS 66/S) was used to detect the characteristic absorbance of functional groups grafted on the graphene hybrid material. Surface functionalization of CNTs was evaluated by FTIR and XPS. The surface morphology of samples was characterized using a field emission scanning electron microscope (FESEM, JEOL, JSM-7500F) at an accelerating voltage of 15 kV. Formation of the CNT-G/Si hybrid structure was studied using a high-resolution transmission electron microscope (HRTEM, JEOL, JEM2100F). Electrical properties were examined using a Keithley 4200-SCS semiconductor analyzer.

### 3. Results and discussion

#### 3.1. Characterization of SAM-G/Si

XPS was employed to check the surface functionalization of graphene film. Figure 2 shows survey scan spectra collected from G/Si, UV-G/Si and SAM-G/Si (figures 2(a), (c) and (e)). The most prominent peaks were C1s and O1s for all sample scans. However, the appearance of an N1s peak centered at 401 eV was observed only for SAM-G/Si (figure 2(e)). In addition, C1s and O1s peaks were fitted by the deconvolution procedure as shown in figure S1 (available at [stacks.iop.org/STAM/15/015007/mmedia](http://stacks.iop.org/STAM/15/015007/mmedia)). Nevertheless, as associated to their intensities the variations of core peak

position were not so large for each of them and it would be difficult to analyze components quantitatively. In the meantime, the C/O ratio for G/Si was 1.6, whereas after UV-treatment, it decreased to 1.4, suggesting an increase of oxygen-containing moieties on UV-G/Si. But, after SAM fabrication on a UV-treated sample, the C/O ratio increased up to 2.2, indicating the increase of carbon-containing molecules can be attributed to the carbons of SAM. Therefore, the XPS study confirmed the transformation of functionalization after surface treatment and signifies the presence of the amine-terminated SAM on the graphene surface [24], which demonstrated that UV treatment provided an efficient surface on graphene for SAM fabrication.

Next, Raman analyses of SAM-G/Si were performed and compared with G/Si, and UV-G/Si as shown in figure 2. The G peak for G/Si was observed at  $\sim 1595 \text{ cm}^{-1}$  (figure 2(b)), which arose from the high-frequency E<sub>2g</sub> phonon mode [25]. The 2D peak, observed at  $\sim 2693 \text{ cm}^{-1}$  (from excitation at 514 nm), was a second-order vibration caused by the scattering of two phonons [26]. Changes of the G peak after UV irradiation and SAM fabrication are shown in figures 2(d) and (f), in which the G peak shifted from 1595 to  $\sim 1592 \text{ cm}^{-1}$ . After SAM deposition, the G peak moved  $\sim 2 \text{ cm}^{-1}$  toward the lower energy region. The 2D peak also shifted from  $\sim 2693 \text{ cm}^{-1}$  to lower energy by  $\sim 3 \text{ cm}^{-1}$  after UV irradiation and further shifted  $\sim 4 \text{ cm}^{-1}$  lower after amine-SAM fabrication which might be adapted n-type

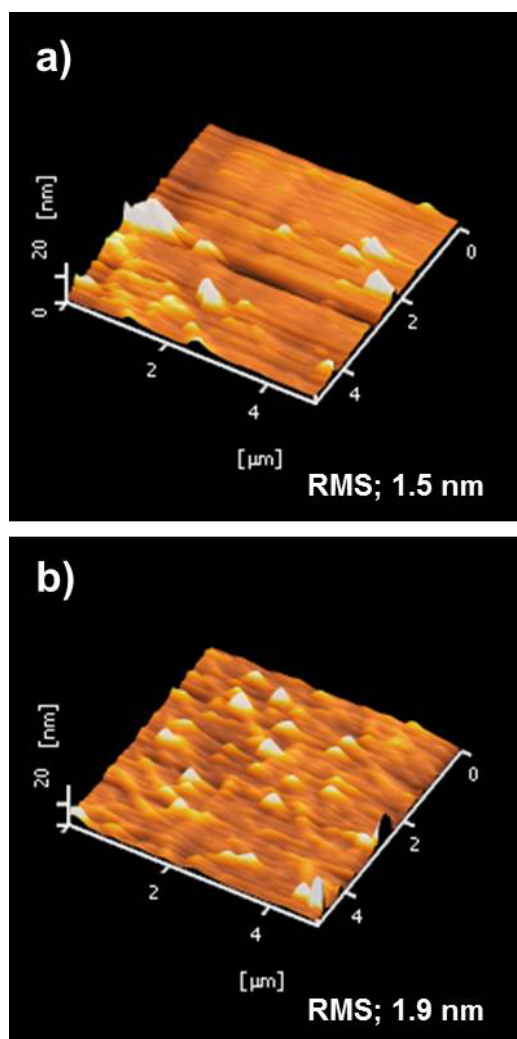


**Figure 3.** AFM topography for G/Si (a) and SAM-G/Si (b).

behavior due to n-doping induced by SAM (figure 2(f)). Das *et al* [27] demonstrated that n-doping of graphene caused the 2D Raman band to shift downward. Typically, n-type doped graphene or adsorption of molecules with electron-donating groups, G band downshifts [6]. In this study, shifts of the G and 2D peaks in the same direction after surface treatment were observed. However, the intensity of the 2D band decreased after functionalization, due to the interaction with functionalized molecules, which clearly indicate an increase of functional sites on the graphene surface. Thus, the molecular conformation has changed from trans to cis due to surface functionalization, which causes interactions between graphene and the functionalized groups [28].

AFM measurements were performed in the tapping mode to characterize surface topography changes of graphene film before and after SAM fabrication as shown in figure 3. A useful description of surface topography was given by the surface roughness [29]. The AFM image of G/Si displayed a lower root mean square (RMS) value (1.5 nm) and non-uniform islands that come from a low level of functional group [30] as shown in figure 3(a). From the

micrographs, it was noticeable that the surface topography of SAM-fabricated graphene film was quite uniform and homogeneous; however, a higher rms value (1.9 nm) was observed as shown in figure 3(b), indicating the existence of substantial functional groups. It was expected that the SAM-G/Si film would be thicker than G/Si as a result of surface functionalization. Importantly, this result indicated that control of the-functionalization density by changing the extent of UV-treatment might be useful. These AFM results were in agreement with the XPS and Raman analyses.

### 3.2. Characterization of acid-treated CNTs

The surface-functionalized CVD graphene film was used to bind surface-modified CNTs. The acid functionalized CNTs were checked by Raman spectroscopy, XPS and FTIR, and spectra from pristine CNTs were used as a reference. For both CNTs samples, D ( $1350\text{ cm}^{-1}$ ), G ( $1594\text{ cm}^{-1}$ ) and 2D ( $2695\text{ cm}^{-1}$ ) bands were seen as shown in figures S2a and S2c (supporting information S2 available at [stacks.iop.org/STAM/15/015007/mmedia](http://stacks.iop.org/STAM/15/015007/mmedia)). However, the spectrum of acid-treated CNTs showed a strong D peak attributable to significant structural defect sites formed from oxidation [31, 32]. Meanwhile, raw XPS data for both samples were analyzed to determine peak locations as shown in figures S2b and S2d. Aside from the main C=C peak at 284.6 eV, extra peaks at higher binding energies for pristine and functionalized CNTs indicated the presence of carbon atoms bound to other functional groups. The binding energy peak at 286.1 eV for pristine CNTs was attributed to atmospheric oxidation or residual oxides [32]. Similarly, for the functionalized CNT sample, -C-O and -OH-C=O (carboxylic acid) contribute [33–35]. These results are consistent with the Raman measurements as shown in figure S1c. To confirm oxygen containing functional groups, FTIR measurement was employed. FTIR spectra of pristine and acid-treated CNTs are shown in figure S3 (available at [stacks.iop.org/STAM/15/015007/mmedia](http://stacks.iop.org/STAM/15/015007/mmedia)). Pristine CNTs displayed an absorption band at  $3435\text{ cm}^{-1}$ , which resulted from a trace amount of water [36]. The IR spectrum of acid-treated CNTs exhibited additional bands at 1730, 1521 and  $1386\text{ cm}^{-1}$ , which were assigned to C=O,  $\text{COO}^-$  and C-O stretching vibration modes, indicating the coexistence of carboxylic acid and carboxylate groups [37]. Thus, FTIR analysis confirmed the surface functionalization of CNTs.

### 3.3. Characterization of immobilized CNT on functionalized graphene film

CNT immobilized on the SAM graphene surface (CNT-G/Si) was characterized by Raman spectroscopy as shown in figure 4. When compared with acid-treated CNTs and SAM-G/Si spectra (figures 4(a) and (b)), differences in the G ( $1591\text{ cm}^{-1}$ ) and 2D ( $2687\text{ cm}^{-1}$ ) peak widths, positions and their intensity ratio for CNT-G/Si (figure 4(c)) was indicative of CNT hybridization with graphene. It was notable that the D band was prominent after CNT adsorption, which was useful for evaluating the combination state of CNT on the graphene

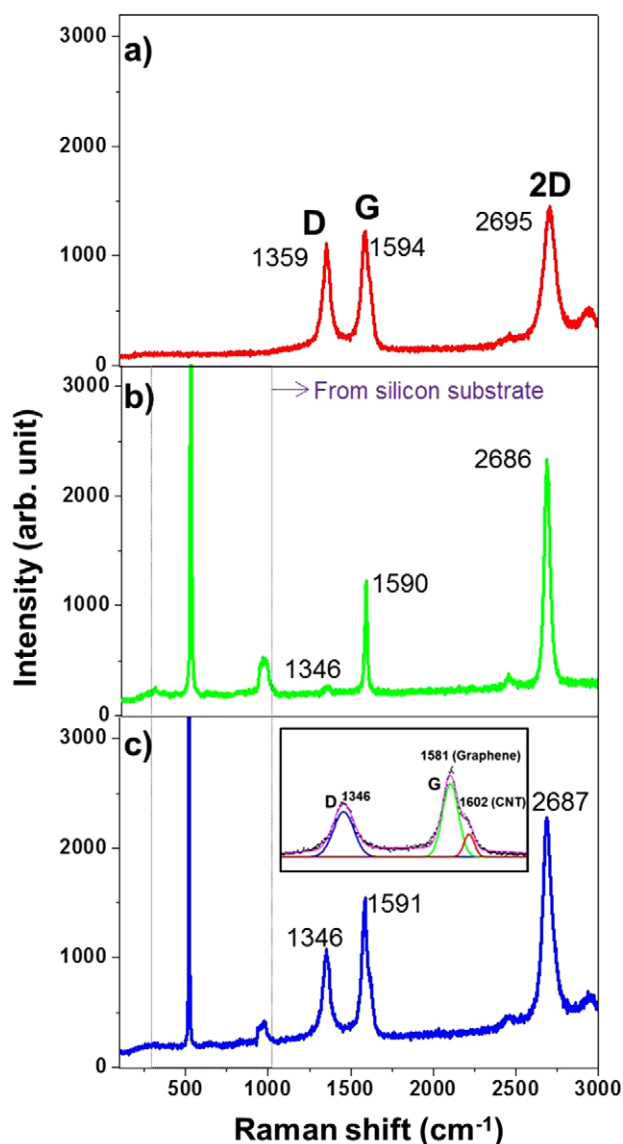


**Figure 4.** Raman spectra for acid-treated CNTs (a), SAM-G/Si (b) and CNT-G/Si (c); (inset; approximation of G peak for graphene and CNT).

surface. Figure 4(a), shows the peak positions of acid-treated CNTs, with G, D and 2D bands at 1594, 1359 and 2695 cm<sup>-1</sup>, respectively, which were all up-shifted compared to the SAM-G/Si bands (figure 2(d)). Moreover, the G and 2D peak positions were lower for CNT-G/Si than for the acid-treated CNTs but higher than for SAM-G/Si. However, these values are lower than for graphene without functionalization with APTES (figure 2(b)) and are indicative of a reduction in the p-type state. Furthermore, core peaks for the D, G and 2D bands were fitted to locate the position of CNT and graphene separately into them as shown in figure 4(c) (inset). But, only the G band has shown a noticeable two peak position as compared to the D band, where lower (1581 cm<sup>-1</sup>) and higher (1602 cm<sup>-1</sup>) shifted peaks appeared that should come from graphene and CNT respectively. Moreover, CNT can be attributed to induce p-type behavior after hybridization.

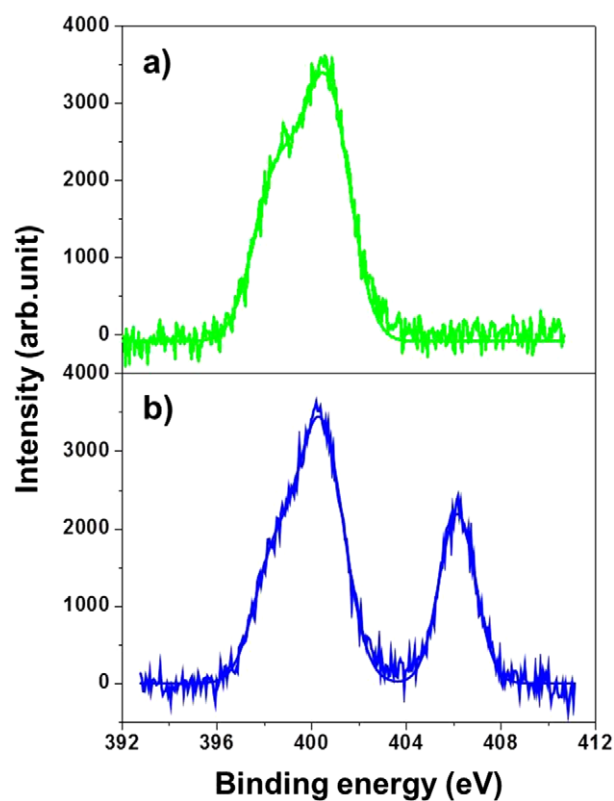


**Figure 5.** N1s XPS spectra for SAM-G/Si (a) and CNT-G/Si (b).

For, p-type doped graphene, or adsorption of molecules with electron-withdrawing groups, it upshifts and softens while it is in contrast for n-type [6]. Likewise, the upshift of the G band position and the downshift of the 2D band position suggests n-doping of graphene, whereas upshifts of the G band and the 2D band positions implies p-doping due to the phonon stiffening effect from charge extraction [27]. Conversely, both G and 2D bands were a bit upshifted after CNT immobilization, with an apparent reduction of the n-type state. However, both n-type and p-type characteristic features might remain in the hybrid material because of chemical bonding between CNT and graphene.

Moreover, the G/D ratio of acid-treated CNTs, SAM-G/Si and CNT-G/Si were found of the order of 1.0, 4.4 and 1.5 respectively, which indicates that the value of the G/D ratio of the SAM-containing sample was reduced after CNT adsorption. This adsorption modulation by immobilization technique was further studied by XPS, FTIR and electrical transport measurements.

Possible binding between CNT and graphene was further performed in an XPS study of the N1s peak (figure 5). For free amines, the N1s peak position was observed at a binding energy of 401 eV (figure 5(a)). The XPS pattern of CNT-G/Si was used to investigate the chemical bonding state. The N1s band appeared at binding energies of ~401 and ~405 eV, after the immobilization reaction (figure 5(b)). This energy split of ~4.0 eV indicates the formation of an amide linkage [38–40] between CNT and graphene as a result of

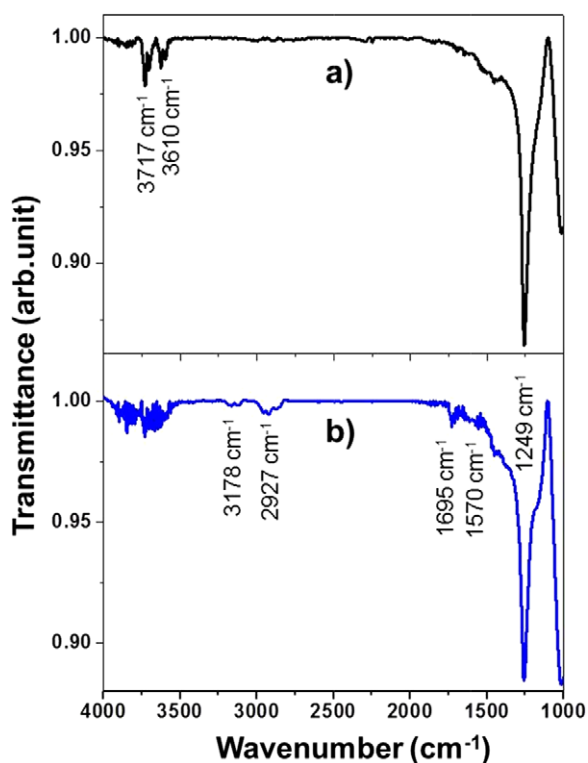
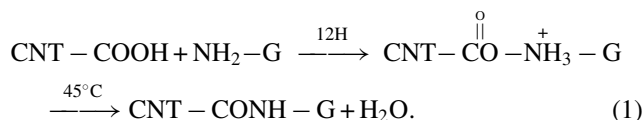


**Figure 6.** FTIR spectra for UV-G/Si (a) and CNT-G/Si (b) (note: G/Si was as a reference).

a chemical reaction as illustrated in the following chemical equation:



To further confirm the presence of the amide functional group (covalent bonding), the FTIR spectra of CNT-G/Si and UV-G/Si, shown in figures 6(a) and (b), were compared. Both samples had a peak at  $\sim 1249\text{ cm}^{-1}$  corresponding to the Si-O bond associated with  $\text{SiO}_2$  film [41]. However, in the spectrum recorded after CNT immobilization, the appearance of new bands at  $1695$  and  $1570\text{ cm}^{-1}$  were assigned to the amide bond C=O stretching ( $-\text{NHCO}-$ ) and the corresponding N-H stretching modes [42]. Moreover, new peaks observed at  $2927$  and  $3278\text{ cm}^{-1}$  were the C-H stretching and N-H bending modes [21, 33, 43] from CNT-G hybridization. However, these characteristic peaks were absent in the UV-G/Si spectrum, which provides strong evidence of covalent CNT attachment onto the graphene surface.

### 3.4. Hybrid structural characterization

The surface morphology of the hybrid material is shown in figure 7. AFM and SEM images illustrated that the CNT was homogeneously distributed onto the SAM-G/Si surface as shown in figures 7(a) and (b). To further characterize the structure of the hybrid material (CNT-G/Si), a sample was examined using TEM (figure 7). The CNT immobilized on SAM-G/Si was found to have an uninterrupted interaction

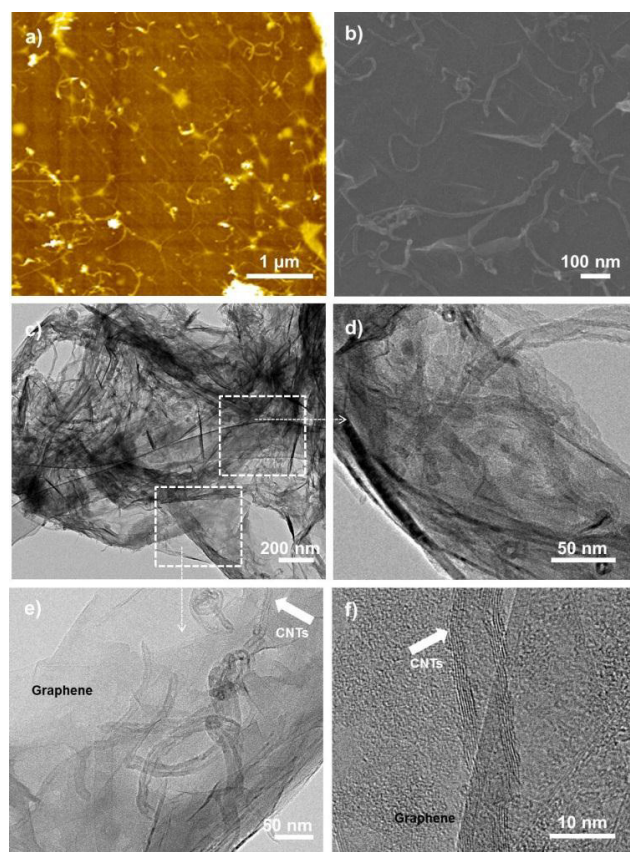


**Figure 7.** AFM and SEM images for CNT-G/Si (a and b) and TEM low and high resolution images (c-e) and (f) (arrows indicate a select region of the hybrid structure).

between CNT and graphene, which clearly showed that CNT was anchored onto the graphene surface as shown in figures 7(c)-(f). The establishment of a uniform, continuous CNT network with graphene might be constructive for promoting hybrid properties.

### 3.5. Field effect transistor (FET) measurement

To validate the n-type and p-type characteristics induced by the chemical binding between the CNT and graphene, FET measurements were demonstrated as shown in figure 8.

Both pristine and hybrid graphene FETs were fabricated on  $\text{SiO}_2/\text{Si}$  substrates using platinum for the source and drain electrodes and 1-butyl-3-methylimidazolium (BmimPF6) as an ionic liquid. The schematic procedure of FET measurements is shown in figure 8(a). The charge neutrality point for G/Si without surface treatment was around zero volts (figure 8(b)) but for CNT-G/Si, two neutrality points located at about  $+1.5$  and  $-1.0\text{ V}$  (figure 8(c)) were indicative of sharp p-n junction behavior with energy separation of the neutrality points within complementary regions. The as-fabricated hybrid device had p-type characteristics due to adsorption of the CNT/graphene surface, while the n-type characteristic was initiated by the amide group as well as insignificant free amine groups, indicating a hybrid property from CNT-G chemical bonding.

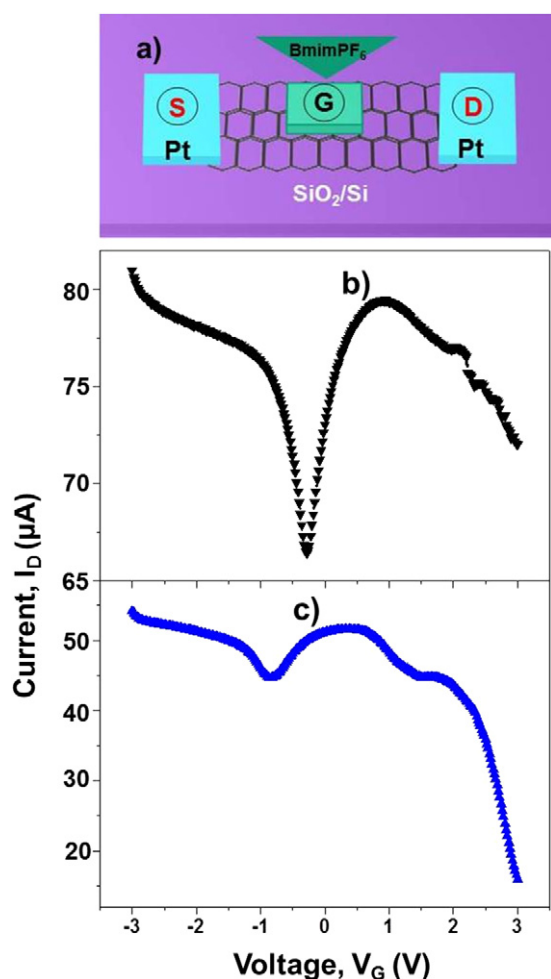


**Figure 8.** Representation of an electrochemically gate-adjusted FETs diagram (a); drain–source current versus gate voltage for G/Si (b) and CNT–G/Si (c).

Based upon the experimental results, the overall synthetic processes of graphene film functionalization (SAM-G/Si) and CNT immobilization onto the aforementioned surface (CNT–G/Si) are illustrated in schematic figure 1. Beyond the fabrication of an amine-terminated SAM on graphene film followed by UV-treatment, a key motivation of this work was the introduction of an active terminal group containing SAM onto CVD graphene film which could be useful to uniformly bind CNTs onto the film surface and to encourage the fabrication of other nanomaterials. Likewise, the presence of an amine group on graphene offers a greater array of potential reactions under mild surroundings; such as the binding of biomolecules, which is normally performed with amine-terminated surfaces [33]. Recently, Yung *et al* [44] reported a unique Pt structure decorated onto a graphene sheet. Various groups have reported that aggregation of CNT on graphene sheets leads to a loss of available surface area and a reduction in supercapacitor performance [20, 45, 46]. The results from the present study reveal a method to produce a uniform and distinctive CNT–graphene structure via covalent bonding, which might be useful in controllably preparing other graphene hybrid assemblies. Because localized SAM

on graphene film can facilitate chemical patterning, an understanding of the amine–CNT interactions may offer a feasible approach to the realization of all-graphene circuits.

#### 4. Conclusions

In conclusion, we have developed a simple, tunable method for the synthesis of covalently bound CNT–graphene hybrid material. UV treatment efficiently provided an effective graphene film surface on which to fabricate SAM. The amine groups on graphene promoted the adsorption of CNTs, leading to the formation of CNT–graphene hybrid material with a unique configuration. Finally, a new class of hybrid material with uniform CNT–graphene networks was demonstrated. This methodology could be of great use in the fabrication of supercapacitors, flexible hybrid electrodes, p–n junction FET devices, among other future applications.

#### Acknowledgments

This work was supported by the Basic Science Research Program (2012R1A1A2041021) through the National Research Foundation of Korea (NRF) funded by the Ministry of Education, Science and Technology (MEST).

#### References

- [1] Novoselov K S, Geim A K, Morozov S V, Jiang D, Zhang Y, Dubonos S V I, Grigorieva V and Firsov A A 2004 *Science* **306** 666
- [2] Geim A K and Novoselov K S 2007 *Nature Mater.* **6** 183
- [3] Lee C, Wei X D, Kysar J W and Hone J 2008 *Science* **321** 385
- [4] Gilje S, Han S, Wang M, Wang K L and Kaner R B 2007 *Nano. Lett.* **7** 3394
- [5] Eda G, Fanchini G and Chhowalla M 2008 *Nature Nanotechnol.* **3** 270
- [6] Rao C N R, Sood A K, Subrahmanyam K S and Govindaraj A 2009 *Angew. Chem. Int. Edn Engl.* **48** 7752
- [7] Liang J, Xu Y, Huang Y, Zhang L, Wang Y, Ma Y, Li F, Guo T and Chen Y 2009 *J. Phys. Chem. C* **113** 9921
- [8] Wang X, Zhi L J and Mullen K 2008 *Nano Lett.* **8** 323
- [9] Yoo E, Kim J, Hosono E, Zhou H, Kudo T and Honma I 2008 *Nano Lett.* **8** 2277
- [10] Leenaerts O, Partoens B and Peeters F M 2009 *Phys. Rev. B* **79** 235440
- [11] Xu Y X and Shi G Q 2011 *J. Mater. Chem.* **21** 3311
- [12] Kodali V K, Scrimgeour J, Kim S, Hankinson J H, Carroll K M, Heer D, Berger C and Curtis J E 2011 *Langmuir* **27** 863
- [13] Compton O C, Dikin D A, Putz K W, Brinson L C and Nguyen S T 2010 *Adv. Mater.* **22** 892
- [14] Stankovich S, Dikin D A, Compton O C, Dommett G H B, Ruoff R S and Nguyen S T 2010 *Chem. Mater.* **22** 4153
- [15] Valentini L, Cardinali M, Bon S B, Bagnis D, Verdejo R, Lopez-Manchado M A and Kenny J M 2010 *J. Mater. Chem.* **20** 995
- [16] Hossain M Z, Walsh M A and Hersam M C 2010 *J. Am. Chem. Soc.* **132** 15399
- [17] Liu L H, Lerner M M and Yan M 2010 *Nano Lett.* **10** 3754
- [18] Li B, Zhiu L, Wu D, Peng H, Yan K and Liu Z 2011 *ACS Nano* **5** 5957
- [19] Stine R, Ciszek J W, Barlow D E, Lee W D, Robinson J T and Sheehan P E 2012 *Langmuir* **28** 7957

- [20] Yu D and Dai L 2010 *J. Phys. Chem. Lett.* **1** 467
- [21] Tung V C, Chen L, Allen M J, Wassei J K, Nelson K, Kaner R B and Yang Y 2009 *Nano Lett.* **9** 1949
- [22] Li C Y, Li Z, Zhu H W, Wang K L, Wei J Q, Li X, Sun P, Zhang H and Wu D 2010 *J. Phys. Chem. C* **114** 14008
- [23] Li X, Zhu Y, Cai W, Borysiak M, Han B, Chen D, Piner R D, Colombo L and Ruoff R S 2009 *Nano Lett.* **9** 4359
- [24] Adhikari P D, Song W, Cha M J and Park C Y 2013 *Thin Solid Films* **545** 50
- [25] Ferrari A C et al 2006 *Phys. Rev. Lett.* **97** 187401
- [26] Malard L M, Pimenta M A, Dresselhaus G and Dresselhaus M S 2009 *Phys. Rep.* **473** 51
- [27] Das A, Pisana S, Chakraborty B, Piscanec S, Shah S K, Waghmare U V, Novoselov K S, Krishnamurthy H R, Geim A K and Ferrari A C 2008 *Nature Nanotechnol.* **3** 210
- [28] Peimyoo N, Li J, Shang J, Shen X, Qiu C, Xie L, Huang W and Yu T 2012 *ACS Nano* **6** 8878
- [29] Ishigami M, Chen J H, Cullen W G, Fuhrer M S and Williams E D 2007 *Nano Lett.* **7** 1643
- [30] Niall M, Hugo N, Nanjundan A K, Toby H and Georg S D 2013 *Carbon* **54** 283
- [31] Rosca I D, Watari F, Uo M and Akasaka T 2005 *Carbon* **43** 3124
- [32] Adhikari P D, Kim S, Lee S and Park C Y 2013 *J. Nanosci. Nanotechnol* **13** 4587
- [33] Ramanathan T, Fisher F T, Ruoff R S and Brinson L C 2005 *Chem. Mater.* **17** 1290
- [34] Noa L, Xiaomeng S, Tatyana B, Hagai C and Wagner H D 2012 *Carbon* **50** 1734
- [35] Adhikari P D, Tai Y, Ujihara M, Chu C C, Imae T and Motojima S 2010 *J. Nanosci. Nanotechnol* **10** 833
- [36] Zhang Y, Li J, Shen Y, Ang M W and Li J 2004 *J. Phys. Chem. B* **108** 15343
- [37] Sun Y P, Huang W, Lin Y, Fu K F, Kitaygorodskiy A, Riddle L A, Yu Y J and Carroll D L 2001 *Chem. Mater.* **13** 2864
- [38] Mou Z, Chen X, Du Y, Wang X, Yang P and Wang S 2011 *Appl. Surf. Sci.* **258** 1704
- [39] Ma Y, Sun L, Huang W, Zahang L, Zhao J, Fan Q and Huang W 2011 *J. Phys. Chem. C* **115** 24592
- [40] Adhikari P D, Imae T and Motojima S 2011 *Chem. Eng. J.* **174** 693
- [41] Oh T 2005 *Japan. J. Appl. Phys.* **44** 4103
- [42] Zhan Y, Yang X, Meng F, Wei J, Zhao R and Liu X 2011 *J. Colloid Interface Sci.* **363** 98
- [43] Suteewong T, Sai H, Bradbury M, Estroff L A, Gruner S M and Wiesner U 2012 *Chem. Mater.* **24** 3895
- [44] Yung T Y, Lee J Y and Liu L K 2013 *Sci. Technol. Adv. Mater.* **14** 035001
- [45] Yang S Y, Chang K H, Tien H W, Lee Y F, Li S M, Wang Y S, Wang J Y, Ma C C M and Hu C C 2011 *J. Mater. Chem.* **21** 2374
- [46] Cheng Q, Tang J, Ma J, Zhang H, Shinya N and Qin L-C 2011 *Phys. Chem. Chem. Phys.* **13** 17615